Extension of the Electron-Promotion Model to Asymmetric Atomic Collisions*

M. Barat
Institut d'Electronique Fondamentale,† Bâtiment 220, Université Paris-Sud-Centre d'Orsay, 91-Orsay-France

and

W. Lichten
Yale University,‡ New Haven, Connecticut 06520

(Received 13 December 1971)

The electron-promotion model is extended to include asymmetric atomic collisions. Diabatic correlations are made between the limits of united and separated atoms. The effects of core penetration are taken into account. The model is especially applicable to the case of inner-shell promotion. The promotion model agrees with the results of Specht, which show that promotion of electrons occurs when an energy level of one atom matches that of another. A detailed discussion of L-shell excitation is given. The model accounts in detail for the subshell-excitation effects and lack of reciprocity found between target and projectile by Kavanagh *et al.* The effects of outer-shell vacancies are felt in inner-shell excitation through the opening or closing of exit channels. In particular, the "solid effect" opens channels leading to outer-shell orbitals of the projectile. The Kessel model is applied to L-shell excitations in asymmetric collisions. The possibility of exciting both collision partners with nearly matching levels is taken into account. Two parameters are needed to fit the total cross section for excitation as a function of atomic number: the critical internuclear distance for a given pair of atoms and the effective range over which the promotion takes place. The parameters needed to fit the total-cross-section data of Cu on targets of different Z, taken by Kavanagh *et al.*, agree with the differential-energy-loss and x-ray data, obtained by Fastrup *et al.*, and by Saris, from different atoms scattered by atomic argon targets.

I. INTRODUCTION

In 1927, the molecular-orbital (MO) model was created by Hund[1] and Mulliken[2] to form a theoretical basis for molecular spectroscopy. In this model, the electrons were treated as independent particles. An important part of this model was electron promotion,[1,2] in which the principal quantum number of certain MO's is higher in the united-atom (UA) limit than in the separated atoms (SA).

In 1930, Beeck[3] observed sharp thresholds for the ionization of noble gases by impact with alkali-metal ions. Weizel and Beeck[4] interpreted these results in terms of electron promotion, with transitions at crossings of MO energy levels. They thought ionization occurred by Auger-electron emission when the electronic energy was raised into the ionization continuum, either directly during the collision or indirectly, after separation of the atoms has occurred. In 1934, Coates[5] observed similar thresholds in inner-shell-vacancy production and suggested a quasimolecular model to explain his results. Almost two decades after Weizel and Beeck's article, Moe and Petch[6] found Auger electrons in alkali-metal-ion–rare-gas collisions, and verified the indirect-ionization mechanism.

In the past decade, a great deal of progress has been made in understanding the mechanism of heavy-particle collisions by the use of differential-scattering measurements. Among the pioneers in this field were Fedorenko and co-workers in the U.S.S.R.[7] and Everhart's group in the U.S.[8] From a classical point of view, there is a direct correlation between the reduced scattering angle (the product $E\theta$)[9] and the impact parameter b, or, more significantly, the distance of closest approach of the nuclei, R_0. Inner-shell excitation in violent collisions was first studied in symmetric systems (Ar-Ar^+, Ne-Ne^+, Kr-Kr^+). Among the several experimental methods used to investigate this inner-shell excitation were coincidence measurements,[10] which gave simultaneous information about the charge state of both scattered and recoiling atoms, the total energy loss, and the impact parameter (or distance of closest approach). Spectroscopy of ejected Auger electrons,[6,11,12] coincidences between scattered ions and ejected electrons,[13] coincidence between fast and slow ejected electrons,[14] and x-ray spectra from excited atoms[15,16] gave more detailed information about the collision process. More recently, asymmetric collisions were studied and similar processes were found.[12,16–24]

Beeck[3,4] had found that the cross section for excitation was largest when both collision partners had nearly the same atomic number. Weizel and Beeck[4] interpreted this in terms of matching of atomic energy levels. In 1965, Specht[25] measured x-ray production by fission fragments in the 5–

80-MeV energy range for the projectiles. He also found enhancement of excitation, as shown by x rays, whenever there was a matching of *any* inner-shell energy level of the projectile with *any* inner shell of the target atom. Specht also interpreted his results in terms of the quasimolecule formed during the collision. These results have been confirmed and extended by Saris and Onderdelinden.[16] Kavanagh *et al.*,[20] by performing their experiments at much lower projectile energies, were able to find level-matching effects within the subshells of the atoms. Recently, Datz *et al.*[24] have found differentiation of excitation cross sections within the fine-structure levels of a given subshell.

In the case of relatively simple systems, such as $H+H^+$, $He+He^+$, quantitative calculations of charge-exchange probabilities, elastic and inelastic differential cross sections and locations of level crossings can be made from *ab initio* calculations. However, in the case of many-electron systems, such as $Ar+Ar^+$, such calculations are only in their infancy.[26] At present, we must use phenomenological models which can be compared with experimental data in a qualitative or semiquantitative way.

One such approach has been to use the concept of diabatic molecular states.[27] These are made from antisymmetrized products of one-electron MO wave functions, can cross other states of the same symmetry, and can exist in the ionization continuum. Fano *et al.* have extended this model to violent collisions, in which the atomic shells deeply penetrate each other.[28,29] This model assumes hydrogen-molecular-ion (H_2^+) -like MO's. During the collision, a quasimolecule is formed, in which the velocity of inner-shell electrons is much larger than the relative speed of the colliding heavy particles. The promoted electrons are trapped by crossings of promoted-inner-shell MO's with outer-shell MO's. Autoionization usually takes place after the collision, although it may occur in the collision complex in some cases.[12,30] The model gives a reasonable interpretation of energy losses, inner-shell excitation, and characteristic internuclear distances for excitation and perturbation of elastic cross sections.[31] In particular, the prediction of fast Auger-electron emission in hard collisions[28] has been confirmed in detail by several experimental groups.[32] Further confirmation of the predictions of the promotion model have come from observations of x rays in symmetric collisions by Saris and Onderdelinden.[16] They and the Livermore group also have studied x-ray emission in asymmetric collisions.[15,16,19-21] Recently, Fastrup and co-workers have made detailed studies of energy loss and electron promotion in asymmetric collisions.[24]

In atoms and molecules one usually distinguishes among three different types of shells: inner, valence, and Rydberg. The valence shell (for example, 3*s* and 3*p* in Ar) contains the electrons which normally account for the forces between atoms and for optical spectra. Inner shells are closer to the nucleus (for example, 1*s*, 2*s*, and 2*p* in Ar), are normally unaffected by atomic collisions or by chemical bonds, and only participate in x-ray or Auger spectra. Rydberg-shell electrons (for example, 3*d*, 4*s*, 4*p*, etc., in Ar) are in orbitals that are far outside the other shells and are only seen in special kinds of spectra. In certain cases, it is difficult to make hard distinctions among the types of shells. For example, in the H atom, the one electron is a perfect example of all three shells simultaneously. In the alkali metals, the outer electron is both in a Rydberg shell and can be a valence electron simultaneously.

Inner-shell electrons in diatomic molecules see potentials that are close to that of two Coulomb centers. A good measure of this is to compare the subshell splitting (difference of energy within a group of levels with the same principal quantum number) with the difference between energy levels from different shells. If the subshell splitting is relatively small, the molecular wave functions are H_2^+-like (in the symmetric case) and obey the promotion model well.

Likewise, Rydberg orbitals in singly charged molecular ions are close to H_2^+ MO's, both in absolute energy and in location of crossings, as has been found by Rosenthal and Foley[33] in the case of He_2^+. These crossings play an important role in oscillations in the total cross sections for excitation of He by He^+ and in many other systems.[31,34]

The case of valence-shell excitation is more delicate, since the one-electron-promotion energies or splittings between shells are comparable to the subshell splittings. Also, the energies of MO's within the valence shell are often so close to each other, that the configuration interaction can mix electronic states. Therefore only rough, qualitative, and sometimes unreliable predictions can be made from simple MO models for the valence shell.[35] It is better to use *ab initio* molecular-potential curves for a good understanding of collision mechanisms. To treat the nuclear motion properly, it has been found useful to carry out the calculations in a diabatic basis set of states.[27] For a system of constructing such states, see the papers by Smith, O'Malley, Sidis and LeFebvre-Brion, and Andresen and Nielsen.[36]

Almost all theoretical discussions of inner-shell promotions have been limited to the symmetric case. In Sec. II, we shall develop a set of correlation rules and diagrams for diabatic MO's for asymmetric collisions. In addition, we shall take into account the effect of transitions between separated

atomic states that are very close together in energy. Our objective will be to bring together a wide range of experimental data that is accumulating in this active area of investigation.

II. PROMOTION MODEL

In this section, we shall extend the promotion model[28,29] to the asymmetric case. The problem is to construct a correlation diagram which connects the united atom ($R=0$) and separated atoms ($R=\infty$) with MO energy levels. The properties of one-electron wave functions depend on the separability of Schrödinger's equation in elliptic coordinates for the two-center problem, with an electron in the Coulomb field of two nuclei, with charges Z_a and Z_b, respectively. The solutions are of the form

$$\Psi(\vec{r}) = X(\xi)\, Y(\eta)\, e^{im\phi}\,, \tag{1}$$

where $\xi = (r_a + r_b)/R$, $\eta = (r_a - r_b)/R$, ϕ is the azimuthal angle measured about the internuclear axis, r_a and r_b are the distances of the electron from each of the two nuclei, and R is the internuclear distance.

Morse and Stückelberg[37] have described how three quantum numbers arise in the two-center problem: n_1, n_2 and n_3 are the number of nodal surfaces corresponding to roots of the functions in Eq. (1), where $n_1 = n_\xi$, $n_2 = n_\eta$, and $n_3 = n_\phi$. Because the number of nodal surfaces is conserved for all internuclear distances, these quantum numbers are "good". This property was used[37] to make the connection between united-atom and separated-atom states in symmetric systems. Several authors have made this connection in the asymmetric case.[38,39] We shall follow Morse and Stückelberg[37] and take a united-atom state of the single electron with radial quantum number n_r, azimuthal quantum number l, and magnetic quantum number m_l, where the principal quantum number is the sum

$$n = n_r + l + 1\,. \tag{2}$$

Table I relates the UA quantum numbers n, l, and m_l with the elliptical quantum numbers n_1, n_2, and n_3. We assume that, in the separated-atoms limit, the wave function goes to one center (either a or b), with quantum numbers n_1', n_2' and m', which satisfy the equation

$$n' = n_1' + n_2' + m' + 1. \tag{2'}$$

The radial quantum number, which is the number of ellipsoidal nodal surfaces must be the same in both united and separated atoms. Thus

$$n_r = n_1 = n_\xi = n_1'\,. \tag{3}$$

The magnetic quantum number $n_\phi = n_3$ simply represents the number of planar nodal surfaces passing through the internuclear axis.[40] It is the same for united- and separated-atoms limits:

$$n_3 = m_l = m'\,. \tag{4}$$

The parabolic quantum number n_2 is the number of parabolic nodal surfaces. This is equal to the sum of such nodes for both atoms, with the possibility of an additional node occurring between the atoms in the case of *ungerade* functions: either

$$n_2 = n_\eta = l - m_l = n_{2a}' + n_{2b}'$$

or

$$n_2 = n_{2a}' + n_{2b}' + 1\,, \tag{5}$$

which in the symmetric case gives

$$l - m_l \begin{cases} = 2n_2' \text{ in the } \textit{gerade} \text{ case} \\ = 2n_2' + 1 \text{ in the } \textit{ungerade} \text{ case.} \end{cases} \tag{6}$$

For all practical purposes, the present authors have found the following less restricted relation uniquely gives the same results as Eq. (5) or (6) in constructing correlation diagrams. This is

$$n_2 \geq n_2'\,. \tag{7}$$

One starts with the separated-atom states and uses relations (2), (3), and (7) to construct the H_2^+ correlation diagram, which is shown in Fig. 1, which

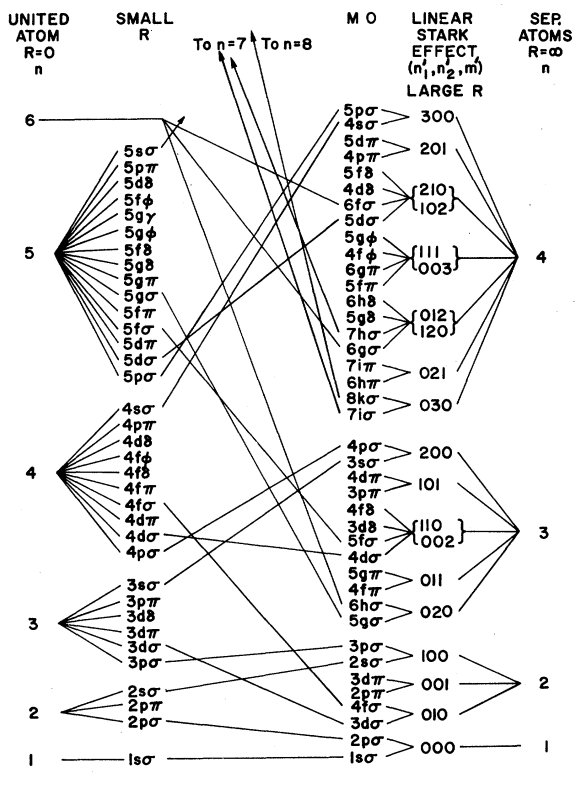

FIG. 1. Correlation diagram for H_2^+. The linear Stark effect upon the order of energy levels is shown both for small and large internuclear distances. For simplicity, only σ MO's are drawn.

TABLE I. Relation between UA quantum numbers n, l, and m_l, and elliptical quantum numbers n_1, n_2, and n_3.

Wave function			Nodal surfaces			
n	l	m_l	n_1	n_2	n_3	Total
1	s	σ	0	0	0	0
2	s	σ	1	0	0	1
2	p	σ	0	1	0	1
2	p	π	0	0	1	1
3	s	σ	2	0	0	2
3	p	σ	1	1	0	2
3	p	π	1	0	1	2
3	d	σ	0	2	0	2
3	d	π	0	1	1	2
3	d	δ	0	0	2	2
4	s	σ	3	0	0	3
4	p	σ	2	1	0	3
4	p	π	2	0	1	3
4	d	σ	1	2	0	3
4	d	π	1	1	1	3
4	d	δ	1	0	2	3
4	f	σ	0	3	0	3
4	f	π	0	2	1	3
4	f	δ	0	1	2	3
4	f	ϕ	0	0	3	3
5	s	σ	4	0	0	4
5	p	σ	3	1	0	4
5	p	π	3	0	1	4
5	d	σ	2	2	0	4
5	d	π	2	1	1	4
5	d	δ	2	0	2	4
5	f	σ	1	3	0	4
5	f	π	1	2	1	4
5	f	δ	1	1	2	4
5	f	ϕ	1	0	3	4
5	g	σ	0	4	0	4
5	g	π	0	3	1	4
5	g	δ	0	2	2	4
5	g	ϕ	0	1	3	4
5	g	γ	0	0	4	4
6	s	σ	5	0	0	5
6	p	σ	4	1	0	5
6	p	π	4	0	1	5
6	d	σ	3	2	0	5
6	d	π	3	1	1	5
6	d	δ	3	0	2	5
6	f	σ	2	3	0	5
6	f	π	2	2	1	5
6	f	δ	2	1	2	5
6	f	ϕ	2	0	3	5
6	g	σ	1	4	0	5
6	g	π	1	3	1	5
6	g	δ	1	2	2	5
6	g	ϕ	1	1	3	5
6	g	γ	1	0	4	5
6	h	σ	0	5	0	5
6	h	π	0	4	1	5
6	h	δ	0	3	2	5
6	h	ϕ	0	2	3	5
6	h	γ	0	1	4	5
6	h	η	0	0	5	5

TABLE I. (*Continued*)

Wave function			Nodal surfaces			
n	l	m_l	n_1	n_2	n_3	Total
7	s	σ	6	0	0	6
7	p	σ	5	1	0	6
7	p	π	5	0	1	6
7	d	σ	4	2	0	6
7	d	π	4	1	1	6
7	d	δ	4	0	2	6
7	f	σ	3	3	0	6
7	f	π	3	2	1	6
7	f	δ	3	1	2	6
7	f	ϕ	3	0	3	6
7	g	σ	2	4	0	6
7	g	π	2	3	1	6
7	g	δ	2	2	2	6
7	g	ϕ	2	1	3	6
7	g	γ	2	0	4	6
7	h	σ	1	5	0	6
7	h	π	1	4	1	6
7	h	δ	1	3	2	6
7	h	ϕ	1	2	3	6
7	h	γ	1	1	4	6
7	h	η	1	0	5	6
7	i	σ	0	6	0	6
7	i	π	0	5	1	6
7	i	δ	0	4	2	6
7	i	ϕ	0	3	3	6
7	i	γ	0	2	4	6
7	i	η	0	1	5	6
7	i	i	0	0	6	6

also shows the linear Stark effect for large internuclear distances. This figure is useful for considering Rydberg orbitals, which are of importance in the case of oscillatory total cross section,[34] as described by Rosenthal.[33]

The major difference between the symmetric and asymmetric case lies in the separated-atom limit. In the symmetric case, the wave function is always an even (g) or odd (u) mixture of separated-atom states. In the asymmetric case, the wave function, in the limit $R=\infty$, is localized on only one atom. Figure 2 shows a correlation diagram for $Z_a \sim Z_b$. As Bates and Carson pointed out,[38] the *effective* number of nodes may change, even if the *actual* number may not. Thus Eq. (5) corresponds to the number of nodes of the separated atomic state of the atom which is correlated correctly to the UA, with an additional set of "phantom" nodes caused by a vanishingly small admixture of a state from the other atom. The present authors have found that the same relations, (2), (3), and (7), uniquely specify the correlation for the asymmetric case, except when two separated atomic states are degenerate. An example of this is shown in Fig. 3, where the $n=1$ level of H is degenerate with the $N=2$ level of

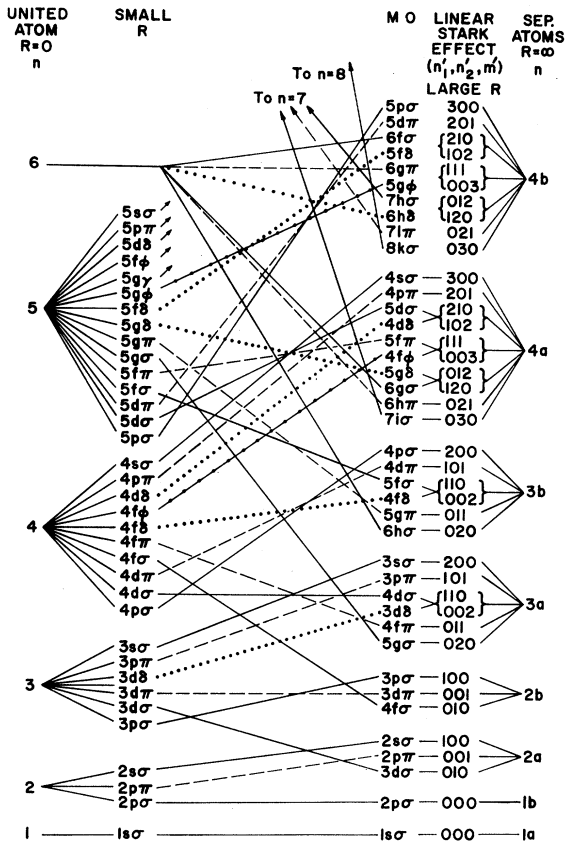

FIG. 2. Correlation diagram for one electron in the field of two nearly equally charged nuclei. Stark effect is shown at small and large R.

He^+. However this degeneracy is lifted by the Coulomb term $-Z_b/R$ for atom a and $-Z_a/R$ for atom b, which makes the levels of the heavier atom higher. Thus the correlation diagram for the asymmetric case can be uniquely constructed, using the same method as for the symmetric case (see Fig. 2). These rules were derived on the basis of properties of the solutions (1) to the differential equations by Gershtein and Krivchenkov.[39]

A correlation diagram for the HeH^{++} molecule is given in Fig. 3. These correlations are suitable for Rydberg orbitals, such as the case of an electron promoted to a highly excited state in a collision involved in a doubly ionized projectile.

A. Crossings and Pseudocrossings

There are three types of crossings in the one-electron systems, both symmetric and asymmetric (see Figs. 1 and 2).

First, it should be noted that the linear Stark shifts of the separated atoms generally are in the opposite direction to that of the promotion. For example, $4f\sigma$, $5g\sigma$, $6h\sigma$, etc. (Figs. 1 and 2) are most strongly promoted. Yet these are the very MO's which are Stark shifted most strongly downward. These opposing effects cause an extensive series of crossings, largely in σ MO's, which are responsible for the Rosenthal effect.[33] In many-electron systems, such as He_2^+, these crossings become pseudocrossings and cause the interference effects which are responsible for oscillations in the total cross section for excitation of Rydberg states.[33] These crossings occur at large internuclear distances, where the Stark effect is relatively large. Apparently, these crossings do not occur in the valence shell, where the Stark effect is quenched by the presence of a large number of easily polarized MO's.

A second type of crossing is caused by the quadrupole field of the two nuclei, near the united-atom case. This causes extensive crossings again, especially in σ MO's, at small values of R. It is not known whether these crossings are present or have any effect in many electron systems, although some indications show them to be present.[26]

It should be pointed out that both types of crossings have been omitted from correlation diagrams for multielectron systems.[28,41]

The third type of crossing is caused by electron promotion, in which the principal quantum number of the united atom is higher than that of the separated atoms. In particular, doubly or multiply promoted MO's, such as $4f\sigma$, $5g\sigma$, etc., are especially effec-

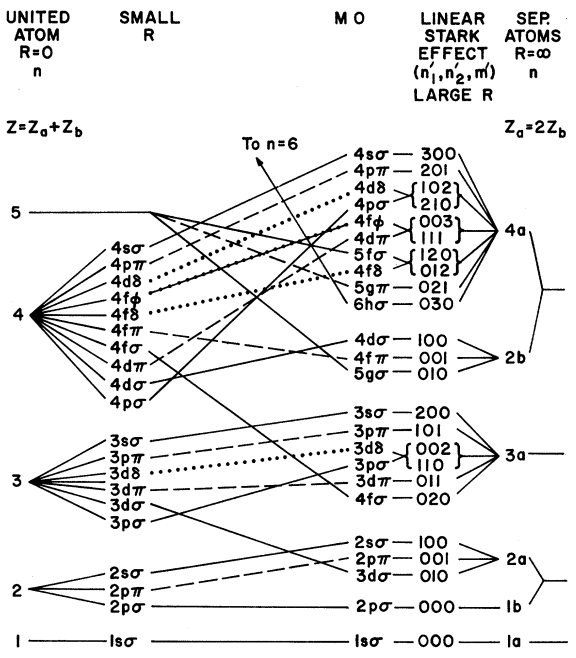

FIG. 3. Correlation diagram for an electron in the field of two nuclei, where one has twice the charge of the other.

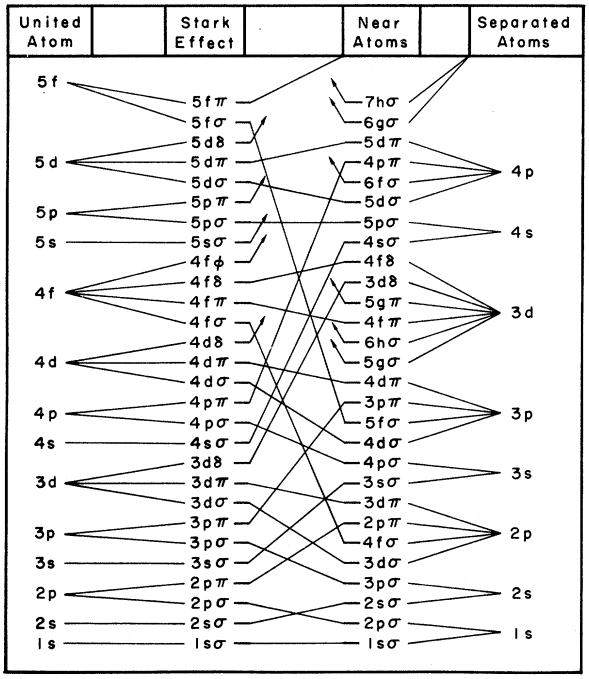

FIG. 4. Correlation diagram for a symmetric, diatomic system with many electrons. This replaces Fig. 3 of Ref. 29.

tive in causing excitation. The bulk of our attention in this article will be directed to this third type of promotion.

Gershtein and Krivchenkov[39] have pointed out a type of pseudocrossing that occurs in one-electron systems. It is possible that, for $Z_a \gg Z_b$, the Coulomb terms $-Z_a/R$ and $-Z_b/R$, which lift the degeneracy between two states (see the sixth paragraph of Sec. II), could actually cause two initially nondegenerate terms to pseudocross. Confirmation of these pseudocrossings has been found by Ponomarev and Puzynina.[42] This type of pseudocrossing seems restricted to one electron systems.

B. Electron Promotion in Many-Electron Systems

In many-electron systems, deviation of the fields of the nuclei from the inverse square law is caused by incomplete shielding or penetration of inner shells by outer-shell electrons. This removes the degeneracy of separated- and united-atom levels of the same principal quantum number. This subshell splitting is shown in Fig. 4 for the symmetric case and in Fig. 5 for the slightly asymmetric case. Neither n_1 nor n_2 is now a rigorously good quantum number. In asymmetric systems, the distinction between u and g orbitals is no longer valid.[43] The result is that crossings are avoided for all MO's with the same value of m, the magnetic quantum number.[43]

In Figs. 4 and 5 diabatic correlations have been made, in which we have followed Refs. 28 and 29 in assuming crossing of promoted MO's. In Refs. 28 and 29 this was justified by the smallness of the subshell splitting relative to the promotion energy. There are two questions. The first, which was not considered in Refs. 28 and 29, applies both to symmetric and asymmetric cases. Why can one assume the subshell splitting to be followed adiabatically by the system near the separated-atoms limit? The answer to this question is given by the discussion of "level crossing" at $R=\infty$,[44] and of the problem of quasiresonant charge exchange. The transition is adiabatic if the collision velocity is small compared to the parameter $2\lambda\Delta E$, where λ is the effective range of the transition from separated atoms to molecular orbitals and ΔE is the subshell splitting (both in atomic units). If $v \gg 2\Delta E\lambda$, the transition is sudden and the atomic fine-structure levels are effectively mixed, according to the appropriate Clebsch-Gordan coefficients connecting MO and fs states.[45]

As for the second question, why, in Fig. 5, are levels like $4f\sigma$ and $3d\sigma$ allowed to cross, when parity is no longer conserved in asymmetric collisions? The answer is that, for small R, the molecular wave functions have a quasiparity.[44]

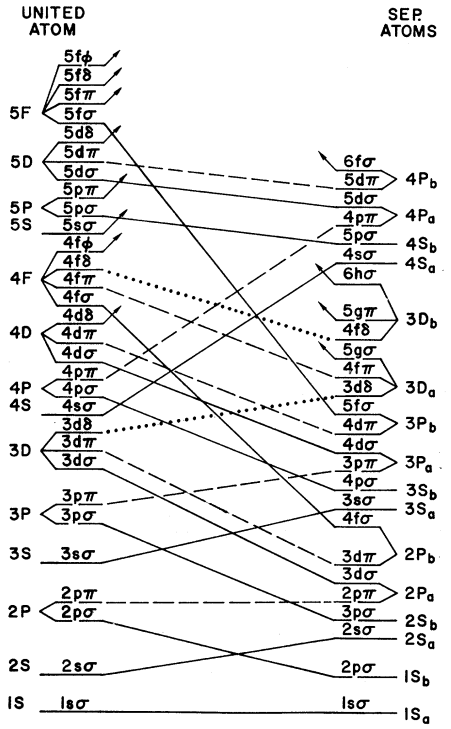

FIG. 5. Correlation diagram for many electrons in the field of two slightly differently charged nuclei.

It is now of interest to construct a correlation diagram in the many electron case, where the individual electrons in both the UA and SA limits now have definite values of the total quantum number n, the orbital angular momentum l, and the magnetic quantum number m. We have seen that the quantum numbers $n_1 = n_r$ and $n_3 = m$ are exactly conserved in the one-electron case, and are thus approximately conserved in the diabatic approximation in many electron systems, as previously discussed in this section and elsewhere.[28,29] Then, according to Eq. (2), *a* MO *must have the same values of the difference* $n - l$ *in both the* UA *and* SA *limits*. This simple relation is sufficient for drawing correlation diagrams (Figs. 4 and 5). For example, in Fig. 5, $1s_a$ ($m=0$, $n=1$, $l=0$, $n-l=1$) correlates with the same values of n, l in the UA, while $1s_b$ correlates with the UA orbital $2p\sigma(m=0,\ n=2,\ l=1,\ n-l=1)$. It is interesting to note that neither n nor l are good quantum numbers, in that both change when there is electron promotion, but the difference $n-l$ is the same in both UA and SA.

C. Swapping

In the one-electron case of asymmetric systems, there are always exactly degenerate levels in the SA. This is because the nuclear charges Z_a and Z_b are both integers. Thus there always are quantum numbers, n_a and n_b, such that the hydrogenic energy levels $-Z_a^2/n_a^2$ and $-Z_b^2/n_b^2$ are equal. For example, in the case of HeH^{++}, the He^+ $(2, 4, 6, 8 \cdots 2n)$ levels are degenerate with the H$(1, 2, 3, 4 \cdots n)$ levels (see Fig. 3). This causes a "swapping" of correlations for the two atoms. For example, the $3a(He^{++}, n=3)$ and $2b$ (H, $n=2$) levels have been swapped, and the relative order of these levels in the correlation has been changed (compare Figs. 3 and 4).

In the case of many-electron systems, swapping takes place when two SA energy levels with the same values of m and $n-l$ change their relative order on an energy-level diagram. This gives us an extremely simple rule for constructing correlation diagrams: *Start with the correlation diagram for nearly equal atomic numbers* (Fig. 5). *Move the levels to the correct relative order* for the case in question. *Swap the correlations for any two levels which change their relative order, if both have the same values of* m *and* $n-l$. An example of such a "swapped" correlation diagram is given in Fig. 6.

D. Electron Promotion in Asymmetric Atomic Collisions: Some General Questions

Our analysis of specific cases will be made clear, if we first discuss a few general questions, in connection with the promotion model.

(i) Why do light particles, such as protons and α particles act only through Coulomb excitation and not through electron promotion? It is a well-known fact that excitation of inner shells by protons and α particles can be calculated to good accuracy by merely treating them as charged particles which excite through the action of their Coulomb fields in the same fashion as electrons.[46]

The reason for this can be seen by examining the energy-level diagram (see Fig. 7). The K-shell H and He electrons are above (higher in energy than) the $2p$ levels for all atoms in which the $2p$ electron can properly be called "inner shell" (for $Z \geq 11$, Na). The situation is the same for other shells (see Fig. 7). Thus protons and α particles cannot excite *any* inner-shell electrons via a promotion mechanism.

(ii) Why are there sharp thresholds for excitation of electrons by heavy-atom collisions? This can be explained in terms of molecular energy levels.[3-5] Figure 8 shows the energy levels of a slightly asymmetric collision pair, K + Cl. Certain energy levels, such as $2p$ Cl, are multiply promoted over a very narrow range of internuclear distances. As the projectile energy is raised, the internuclear distance in head-on collisions suddenly diminishes below the critical distance, the promoted electron crosses levels of excited states, and excitation via radial coupling occurs. This mechanism holds for symmetric as well as asymmetric collisions.[47] Other electrons, such as $2s$

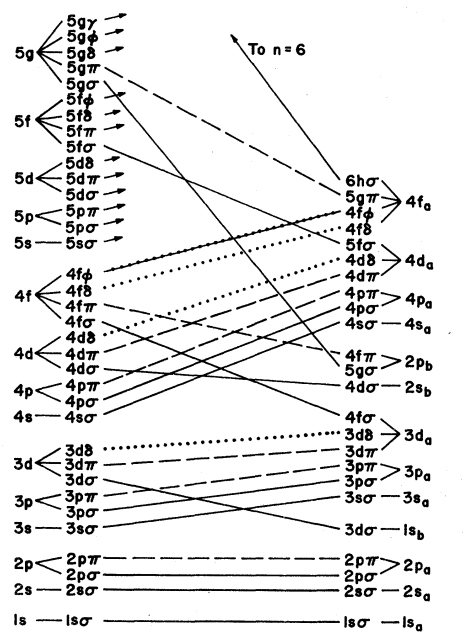

FIG. 6. Correlation diagram for two different atoms, with swapping.

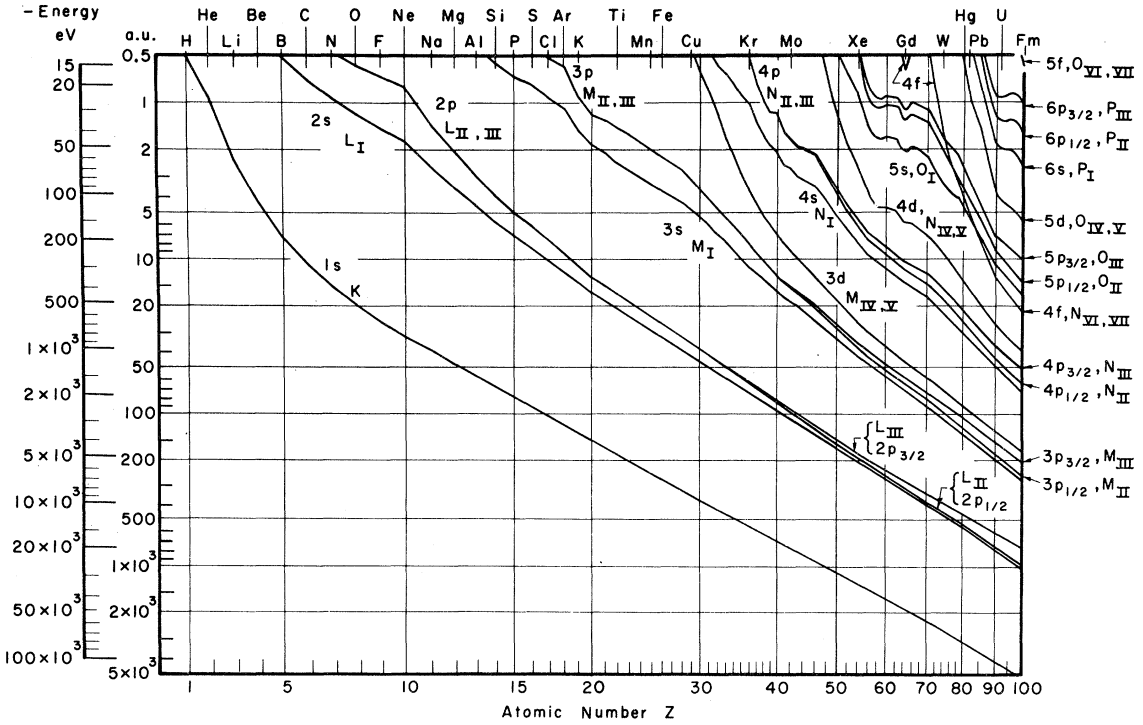

FIG. 7. Energy levels of inner shells of atoms. Source: $1 \leq Z \leq 41$, J. C. Slater, *Quantum Theory of Atomic Structure* (McGraw-Hill, New York, 1960), Vol. I, p. 206; $42 \leq Z \leq 100$, T. A. Carlson, C. C. Lu, T. C. Tucker, C. W. Nestor, Jr., and F. B. Malik, Oak Ridge National Laboratory Report No. 4614 (unpublished) (available from National Technical Information Service, Springfield, Virginia 22151, for $3.00); see also, C. C. Lu, T. A. Carlson, F. B. Malik, T. C. Tucker, and C. W. Nestor, Jr., At. Data 3 (No. 1), 1 (1971). Energy levels of different atoms can be compared by drawing horizontal lines across this drawing.

Cl, are excited by singly promoted MO's via a rotational coupling mechanism ($3p\sigma$ to $3p\pi$ in this example), which is not as sharp, since the transitions occur over a wider range of internuclear distances.[47]

(iii) Why do cross sections for excitation reach a maximum for atomic numbers where energy levels of collision partners match each other? The work of Specht and others[16,20,21,24,25] has shown the importance of level matching in electron promotion. (In symmetric systems, the levels are automatically matched by nature, so the question never arises.)

The promotion model again gives a specific answer to this question. Let a projectile of fixed energy and atomic number bombard targets of different atomic number Z. As Z is increased, electron promotion in the projectile will begin to occur for that value of Z for which swapping occurs. In particular, swapping will take place whenever two levels of the same value of $n-l$ change order in the energy-level diagram (Fig. 7), i.e., the combinations $1s$-($1s$, $2p$, $3d$, etc.), $2s$-($2s$, $3p$, $4d$, etc.), $2p$-($1s$, $2p$, $3d$, $4f$, etc.), etc. According to the strict rules of the correlation diagrams, the cross section for inner-shell excitation should rise discontinuously from zero to a large value, as soon as the atomic number Z reaches the swapping point. Because of the relative motion of the two nuclei, there will be a quasisymmetrical promotion for a range of values of Z around the swapping point. At the swapping point, the excitation will be equally shared between the two collision partners. The range of atomic numbers is given by the uncertainty principle (Massey criterion).[48]

The cross section should rise to a maximum only slightly beyond the swapping point, since the cross section for excitation of either collision partner decreases with increasing Z and fixed kinetic energy. There are several reasons for this decrease. First of all, as the atomic number of the united atom increases, the larger nuclear charge will draw in the radius of the crossing points (where excitation takes place) and lower the cross section. Secondly, as the nuclear repulsion between atoms increases, the cross section rapidly falls off with increasing Z. The falloff becomes very fast as the threshold is reached. Finally, in many cases, the number of open channels for reaction is de-

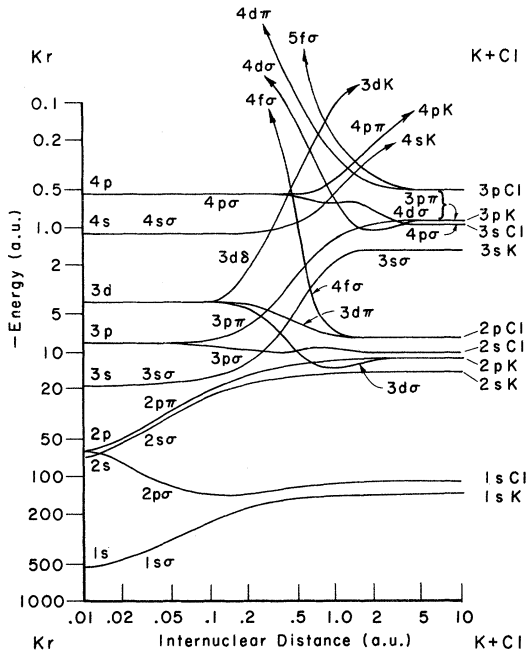

FIG. 8. Energy levels of a slightly asymmetric diatomic system, KCl. Levels of united-atom and separated-atom limits are obtained from references given with Fig. 7. Other energies are estimated by the present authors.

creased, as the outer shells fill up with electrons with increasing target Z. (For solid targets, the latter argument only holds when promotion is to empty shells of the target atom.)

These arguments can be applied to the reversed case of fixed target atom, with variable Z in the projectile, except for solid or dense targets, or other causes of excitation or ionization of the projectile. These are discussed in Sec. II E.

E. Outer-Shell Excitation Effects—"Solid Effect"

One question that often arises is: Should the energy levels of the neutral atom or of the incident ion be used for constructing energy level and correlation diagrams? The motivation behind this question lies in the shift in atomic energy levels as the atom is ionized. Our answer to this question is that the state of the outer shell should have little effect on the promotion of inner shells. The reason is that promotion takes place at small internuclear distances where both target and projectile inner shells share the same environment. Therefore, the levels of the neutral atom seem as good as any for constructing correlation diagrams.

The most convincing experimental evidence for this point of view is the work of Kessel, McCaughey, and Everhart[10] for K-shell excitation with Ne^{++} projectiles on neutral-neon-gas targets. The Doppler-shifted electron spectra show equal K-shell excitation for target and projectile. Since the energy levels of Ne^{++} are shifted about 40 eV below those of Ne, one might expect preferential promotion of the neutral K-shell electron. Since this is not the case, we conclude that the unshifted levels of the neutral atoms are the best for theoretical studies of inner-shell promotion.

A related question is whether the Coulombic shifts of energy levels, caused by the fields of the partner's partially shielded nucleus, would not cause a swap in the correlation diagram in a very asymmetrical collision. (See the discussion at the end of Sec. II A and Refs. 40 and 42 for a discussion of the effect.) Although this possibility cannot be ruled out, the effect is small, of the order of a few atomic units, in most cases. This amounts to a change of only one or two units of atomic number, an effect that would be masked by nuclear-motion-induced smearing out of the swapping point. Thus it is difficult to find a clear-cut case where this effect would be observable.

Outer-shell excitation or ionization has a very great effect on exit channels.[29] The probability of transfer of a promoted MO to a final excited state is roughly proportional to the number of vacancies in the shell of final destination. These vacancies can be produced by ionization or excitation.

Strongly promoted MO's, such as $4f\sigma$ ($2p$ in SA $\rightarrow 4f$ in UA) in $Ar+Ar^+$ collisions or $6h\sigma$ ($3d$ SA $\rightarrow 6h$ UA) in $Kr+Kr^+$ collisions, do not seem to be affected strongly by outer-shell excitation or ionization. These MO's seem to have no shortage of outer-valence-, Rydberg-, or even continuum-shell channels for dumping promoted electrons.

On the other hand, K-shell excitation usually occurs via a singly promoted $2p\sigma$ MO (see Fig. 5 or 8), which is excited by rotation of the internuclear axis and ends in the $2p$ shell of the heavier collision partner. Here the number of vacancies is critical.[29]

McCaughey *et al.*[49] found that the K-shell promotion probabilities in (Ne, Ne^+, or Ne^{++}) collisions with Ne targets were in the ratios 2:1:0.6, in partial agreement with the theoretical values[29] of 2:1:0. It is not known whether the disagreement in the case of neutral Ne is due to excitation of the atoms during neutralization, or to a breakdown in the molecular approximation. Both are possibilities at the high velocities ($\frac{2}{3}$ a.u.) of a 200-keV Ne beam.

Since the molecular model predicts no $2p$ vacancies in $Ar+Ar^+$ collisions at 1.5 MeV, the K-shell excitation found by Kessel *et al.*[10] is clear evidence of breakdown of the molecular approximation at these high energies (velocity > 1 a.u.).

Orgurtsov *et al.*[12] have found a much lower cross section for fast electrons formed in very slow 15-keV Ar^+ on Ne than in equally slow 7.5-keV Ne^+ on

Ar. They interpret the $Ne^+ + Ar$ excitation in terms of a transfer of an Ar($2p$) electron to the empty $2p$ level of Ne via the $3d\sigma$-$3d\pi$ rotationally induced transition, whereas in the $Ar^+ + Ne$ collision, this channel is closed. It is interesting to note that the $3d\sigma$-$3d\pi$-$3d\delta$-$3d$ Ar channel is open in both cases. Perhaps at this low velocity, the double-quantum transition $3d\sigma \rightarrow 3d\delta$ has a low probability. Perhaps at higher velocities, this channel would open, more nearly equalizing the two cross sections.

Fastrup *et al.*[13,24,50] have reported data on K-shell excitation which are a more unambiguous test of the promotion model. Here, variation of the atomic number of the target or projectile affected the exit channels. The larger the atomic number of the heavier atom (as in the C^+, N^+, O^+, Cl^+, Ne^+, Na^+ series), the smaller the cross section for K-shell promotion, which occurs almost entirely in the lighter atom, in agreement with the promotion model. These experiments have been an excellent test of the effects of closing or opening of exit channels on excitation cross sections. In particular, the use of Na^+ projectiles on Ne targets eliminates the objectionable features of the Ne + Ne system.[49] They found less than 1% of the collisions resulted in K-shell promotion, in agreement with the promotion model. Lorents and Conklin, and Francois *et al.*[35] also have studied K-shell excitation in the $Li^+ + He$ system. The results were interpreted[35] in terms of the promotion model. Similar results were found by Der *et al.*, where excitation of the C^+ K shell increases in going from Ne^+ to C^+ projectiles (see Fig. 9).[19]

In the case of solid targets, a distinction was made by Saris and Bierman[16] between target and projectile atoms. Projectile outer-shell, and possibly some inner-shell, electrons can be excited or lost during the atom's passage through the solid. This is not true for the target atom. This "solid effect" is partly due to the asymmetrical condition of the exit channels in target and projectile.[16]

Saris and Onderdelinden[16] found that L-shell x ray yields doubled above threshold, while Auger yields remained constant in the experiments of Rudd and co-workers.[51] Saris and co-workers interpreted this as a small change in the Auger yield caused by outer-shell excitation.[16] Since the x-ray yield is only 1%, a very small change in the Auger yield changes the x-ray results by a factor of 2. Caution in interpreting x-ray data as a quantitative measure of excitation is thus indicated.

III. CASE OF L-SHELL EXCITATION

In this section, we examine in detail experimental results of L-shell excitation as an application of the extended promotion model. Because of the complexity of factors affecting experimental results (see Sec. II E for example), a quantitative calculation of cross sections will not be tried. On the other hand, experiments can be used to extract rather precise parameters of the molecular systems. Comparison of the parameters obtained from quite different experiments will furnish a test of the model.

A. Argon Targets

Everhart, Afrosimov, and their co-workers[7,8,10] have investigated energy losses in $Ar^+ + Ar$ collisions; Rudd, Ogurtsov, and their co-workers and others have studied Auger-electron emission.[11–13] Saris and Orderdelinden have observed x-ray emission (see Fig. 12) and Fastrup and co-workers[17] have studied energy losses and electron emission in collisions of projectiles of different atomic numbers with argon targets. The relative position of the atomic number of the colliding partner of the argon atom plays a prominent role in the discussion of experimental data. Accordingly, we shall discuss the data within the framework of the relative atomic numbers.

1. *Heavier Partners, $Z > 18$ (Available Experimental Data:* K^+, Ti^+, Mn^+, Fe^+, *and* Cu^+ *on* Ar)

In these cases, the correlation diagram in Fig. 5 is appropriate, in which Ar is atom b and the

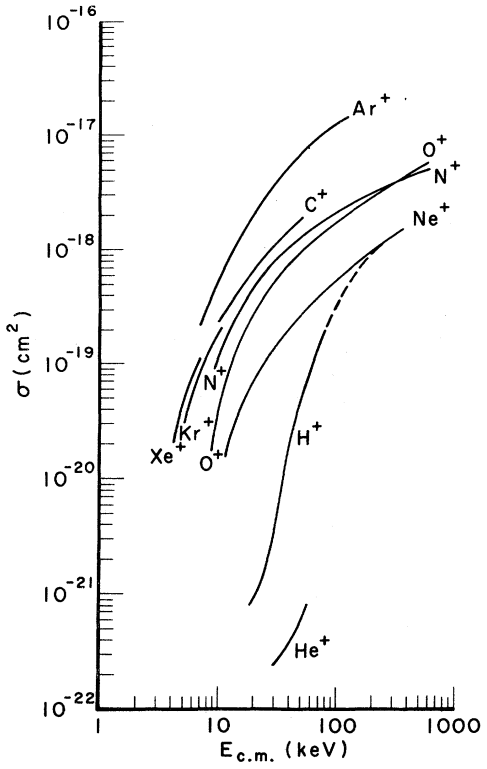

FIG. 9. Cross sections for K-shell excitations in a carbon target. Source: Ref. 20.

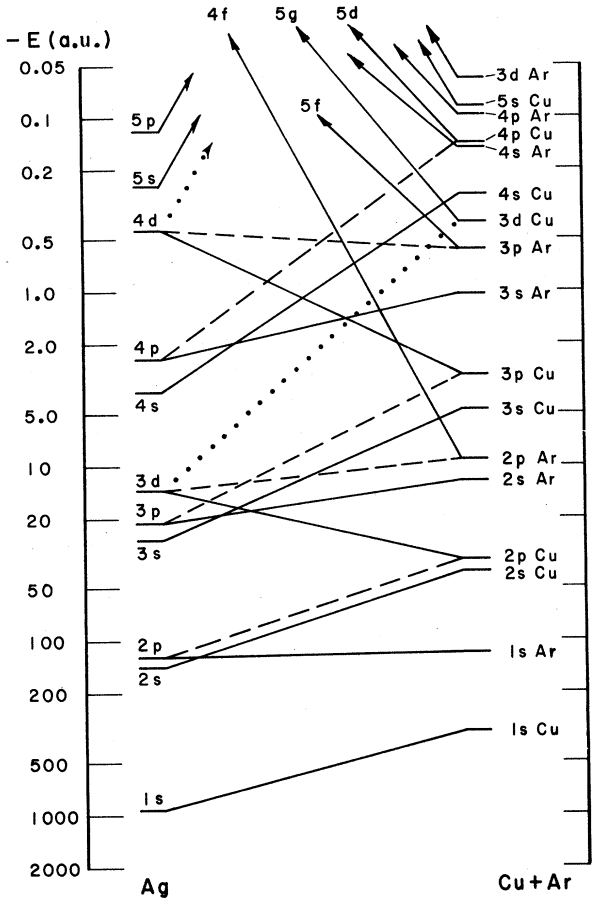

FIG. 10. Correlation diagram for copper-argon. σ states, solid line; π states, dashed line; δ states, dotted line.

heavier projectile is atom a. It is also instructive to examine Figs. 8 and 10, which are typical for these collisions, and to compare these with Fig. 4 of Ref. 29. At this point, it is important to remember the prominent part played by the $4f\sigma$ MO in Ar L-shell excitation in $Ar+Ar^+$ collisions.[28,29] This is because of the crossing of this MO with several MO's which go to $n=3$, 4 levels of the UA and SA.

For $Z \geq Z_{Ar}$, we must correlate the Ar $2p$ atomic orbitals (AO) ($L_{II,III}$) with the $4f\sigma$ (Figs. 8 and 10). With the exception of K^+ projectiles, the experiments of Fastrup *et al.*[17] show that all the L-shell excitation goes into the lighter lower-Z Ar atom, in accordance with the correlation diagram. Fastrup *et al.*[17] also found that the "active distance" of closest approach became smaller as Z was increased ($R_0=0.23$ Å for $Ar+Ar^+$; $R_0=0.186$ Å for $Ar+Mn^+$). This is in agreement with the expectation of decreased L-shell radius with increased nuclear charge of the collision partner or, equivalently, of the united atom.

For values of atomic number Z near 18, the L-shell energies of both partners become nearly the same and a quasiresonant exchange of L-shell excitation occurs, as discussed in Sec. IID (iii). In K^+ ($Z=19$) + Ar collisions, Fastrup *et al.*[17] found about 25% of the L-shell promotions result in excitation of the heavier nucleus. Presumably, the results are about the same in $Cl^+(Z=17)$ + Ar collisions. For $Ar+Ar^+(Z=18)$, the excitation must divide equally. This is in reasonable agreement with the results of Saris *et al.*,[16] who found about a 50% drop in Ar L-shell x-ray excitation in going from Ar^+ to Cl^+ projectiles.

The excitation of the $2p(L_{II,III})$ electrons of the heavier partner should occur via the $3d\sigma$, $3d\pi$, and $3d\delta$ MO's at smaller internuclear distances (see Fig. 8). Fastrup *et al.*[17] did not observe these transitions, presumably because their experiments were done at larger values of internuclear distance, in the triple peak region ($R \sim 0.5$ a.u.).

2. $11 \leq Z \leq 16$ (Al^+, P^+, *and* S^+ *on* Ar)

As in the previous case, we expect that the $4f\sigma$ MO correlates with the L shell of the atom with smaller Z. Therefore excitation should take place exclusively in the L shell of the lighter atom (see Figs. 5, 8, and 11), in agreement with the results of Fastrup *et al.*[17] On the other hand, Saris has reported a small cross section for Ar L-shell emission in Al^+ + Ar collisions.[16] These excitations arise from the same $3d\sigma \rightarrow 3d\pi \rightarrow 3d\delta$ promotion. The experiments of Saris *et al.*[16] are total-cross-section measurements, which give results of collisions integrated over all internuclear distances, which accounts for the difference in the two sets of results.[16,17]

3. $6 \leq Z \leq 10$ (C^+, N^+, O^+, *and* Ne^+ *on* Ar)

The $2p$ shell begins to open as the collision partners become lighter than Na^+ ($Z=11$). Therefore a new set of possibilities is expected for Ar L-shell excitation (see Figs. 5, 8, and 11) via the $3d\sigma - 3d\pi$ coupling mechanism.[52] For the reasons mentioned in Sec. IID (iii), we can expect the cross section for excitation of the Ar L shell to reach a new maximum slightly above $Z=6$, where the Ar $2p$ level swaps with the K shell of the lighter collision partner, in good agreement with experiment[16] (see Fig. 12).

The technique of energy-loss measurements has been applied in this region of Z by Kessel[53] for Ne^+ + Ar, by Knystautas *et al.*[54] for N^+ + Ar and by Bingham[18] for O^+ + Ar collisions. These results have several features in common. There is an increase in energy loss as the internuclear distance decreases below $R_0 \sim 0.3$ a.u. The rise is not as abrupt as in the case of the $4f\sigma$ promotion ($Z \gtrsim 18$); it occurs at a much smaller internuclear distance

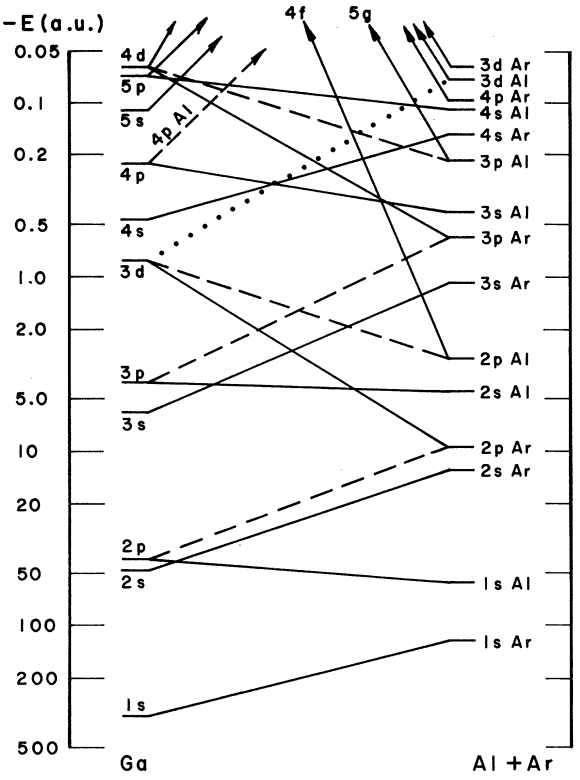

FIG. 11. Correlation diagram for aluminum-argon. See caption to Fig. 10.

and over a wider range of values. As Kessel[53] points out, the excitation is velocity dependent. All these results are in agreement with expectation from the assumption of an excitation via a rotational coupling of the $3d\sigma - 3d\pi - 3d\delta$ transitions. In all respects, the results resemble the second major rise in L-shell excitation, observed by Kessel and Everhart[10] in $Ar + Ar^+$ collisions, which has been previously attributed to the same mechanism.[28,29,55]

Bingham[18] interprets his results to disagree with the promotion model, because the jump in energy loss in $Ar + O^+$ collisions appears to be dependent on R_0, rather than being discrete. However his conclusions are based on only partly resolved experimental results. Until the experiment is repeated under adequate resolution, we feel that his interpretation is premature.

4. $Z \leqslant 5$ (H^+ *and* He^+ *on* Ar)

For $Z < 5$, the Ar $2p$ and partner $1s$ orbitals swap. Now the Ar L-shell electrons are no longer promoted, as discussed in Sec. IID. The possibility of an L-shell excitation via the promotion mechanism no longer exists; the promotion results in excitation of the partner atom's K shell. The cross section for Ar L-shell excitation should fall off very rapidly for $Z < 5$. The results of Saris *et al.*[16] show a very low cross section for Ar L-shell excitation by protons and α particles, in agreement with the promotion model.

B. Heavier Targets and Projectiles

Kavanagh *et al.*[20] have studied Cu L-shell x-ray emission in collisions involving Cu as both projectiles and targets. In all cases, the targets were solids. A very wide range of atomic numbers was chosen and the projectile energy was carefully chosen to enhance the effect of level matching.

The authors[20] noted an apparent subshell effect in their data. The cross section for xenon ($Z = 54$) on Cu *targets* appeared to be near a peak value, corresponding to a match of Cu L-shell levels with Xe $M_{I,II,III}$ binding energies (see Fig. 7). On the other hand, the peak for Cu *projectiles* occurred at $Z \sim 64$ (see Fig. 13), which corresponds to a match of the Cu L shell with target $M_{IV,V}$ levels. The authors[20] raised the related question of the small cross section (see Fig. 13) near $Z_{target} \sim 88$, where Cu L and target $N_{I,II,III}$ energy levels match (see

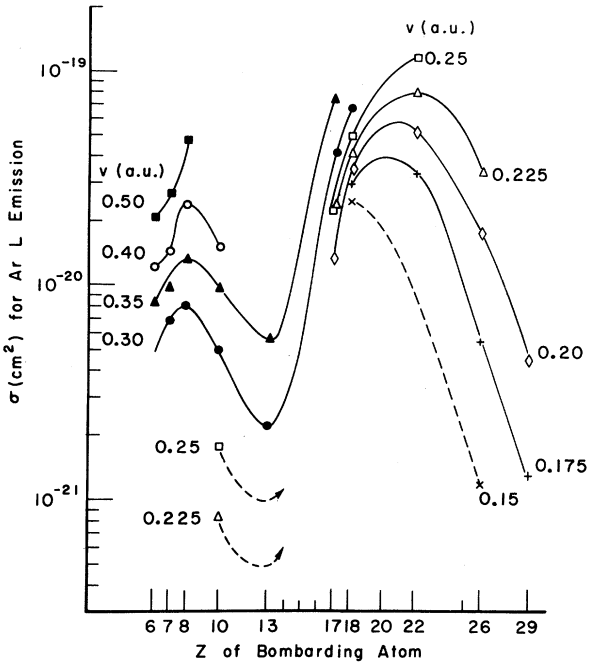

FIG. 12. Cross section for excitation of L-shell x-rays in Ar targets by projectiles of atomic number Z, with relative velocity as a parameter. Note the relatively small dependence on nuclear velocity at $Z \sim 18$, where the excitation mechanism is via a doubly promoted $4f\sigma$ MO, with crossings of many other σ MO's. Compare this with the relatively large velocity dependence at $Z \sim 6$, where the mechanism is by means of a rotationally induced $3d\sigma - 3d\pi$ transition (see Fig. 11).

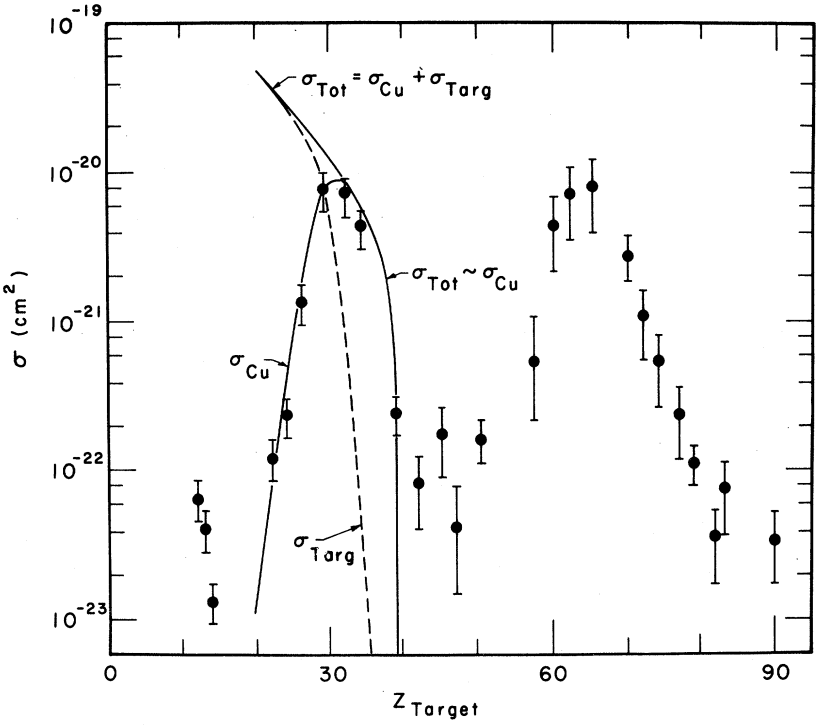

FIG. 13. Experiment cross section for excitation of Cu L-shell x rays in collisions with targets of atomic number Z. The Kessel model gives the curve for the total excitation cross section σ_{tot}. The cross section for exciting copper, σ_{Cu}, is calculated from σ_{tot} by taking into the account the division of excitation between target and projectile atoms. The theoretical fit is only calculated in its range of validity, near $Z=29$. Source of experimental data points: Ref. 20.

Fig. 7).

A very natural interpretation of these results can be made with the promotion model. The peaks at $Z \sim 10$ and 30 occur slightly above the swapping points between Cu L shell and collision partner K and L shells, respectively.

These are entirely analogous to the case of Ar discussed in Sec. III A. The promotion near the (Cu, L; Z, M) shell swapping point is more complex (see Fig. 5, in which b represents Cu and a represents the heavier partner). The L shell of Cu can be promoted by the $3p\sigma$-$3p\pi$ rotationally induced transition, which ends on the $3p$ orbital of the heavier atom.[56] It also can proceed via the $3d\pi \rightarrow 3d\delta$ transition, which ends on the $3d$ level of the collision partner.[56] Finally, it can proceed via the $4f\sigma$ MO which goes to many very highly excited orbitals of both collision partners.[56]

In the case that the Cu atom is the projectile, all the $3p$ and $3d$ AO's of the target atom are filled[56] (for $Z > 29$) and only the $4f\sigma$ promotion mechanism can occur. The maximum cross section for this process should occur slightly to the right of the place where the Cu, $2p$ and Z, $3d$ orbitals swap ($Z \approx 60$, see Fig. 7), in agreement with experiment (see Fig. 13).

With Cu targets, it is possible that the solid effect (see Sec. II E) could open the first two exit channels. This would allow a peak somewhere nearer the (Cu, $2s$; Z, $3p$) swapping point ($Z \sim 56$). The experimental data are incomplete[20]; the excitation at $Z = 56$ is comparable to the excitation at $Z = 60$ in Fig. 13.

The existence of the low cross section at $Z = 88$ (see Fig. 13) is predicted by the promotion model; the Cu L-shell promotion goes via the $5g\sigma$ MO (see Fig. 6). This cross section should be large near the swapping point at $Z \sim 95$, where the (Cu, $2p$; Z, $4f$) AO's match. All other excitation would be to filled orbitals and would not be expected for Cu projectiles.

C. Molecular Parameters

By assuming a screened Coulomb interaction, Everhart,[57] Kessel,[10] and Fastrup[17] and their coworkers have determined the promotion probability for each of the two electrons in the $4f\sigma$ MO as a function of internuclear distance. For almost all of the cases of Ar with a collision partner $11 \leq Z \leq 29$, this probability rises sharply to near unity for $R_0 \lesssim 0.5$ a.u., over a narrow range of internuclear distances, $\Delta R_0 \sim 0.1$ a.u.

Kessel has devised a simple model[51] to predict the total cross section for any inelastic event which depends on this rapid two-electron promotion. It assumes a promotion probability of unity for $R_0 < R_C$ and zero for $R_0 > R_C$, where R_C is the critical internuclear distance where promotion is assumed to occur suddenly. This model predicts a sharp rise of cross section to a limiting value πR_C^2 as a function of energy. This model gives excellent agreement with Auger-electron data[51] in $Ar + Ar^+$

collisions. It gives good results near threshold for x-ray data, but it fails to fit the data at higher energies, as discussed in Sec. II E. (The poorer fit of the excitation data for Ne K-shell x rays[16] in collisions with Ar presumably arises from the different mechanism of excitation, as discussed in Sec. II D.) For Ar+Ar$^+$ collisions, Saris *et al.*[16] obtained a value for $R_C = 0.23$ Å from x-ray data, in good agreement with the value of 0.247 Å of Fastrup *et al.*,[17] obtained from differential-energy-loss data and the value of 0.25 Å obtained by Cacek, Kessel, and Rudd from Auger-electron data.[51] This agreement leads one to hope that reliable parameters of the quasimolecule can be obtained from total and differential cross sections for excitation.

We have fitted the Kessel model[51] to the total cross sections for copper L-shell excitation obtained by Kavanagh *et al.*[20] The effect of quasiresonant mixing of L-shell levels with nearly matching energies was taken into account by setting the excitation probability P_E equal to a product of the Kessel promotion probability P multiplied by a mixing factor M. We gave this factor the correct form to give zero excitation for very light target nuclei, 50% excitation for Cu+Cu collisions, and 100% excitation for very heavy target atoms:

$$P_E = MP,$$

where

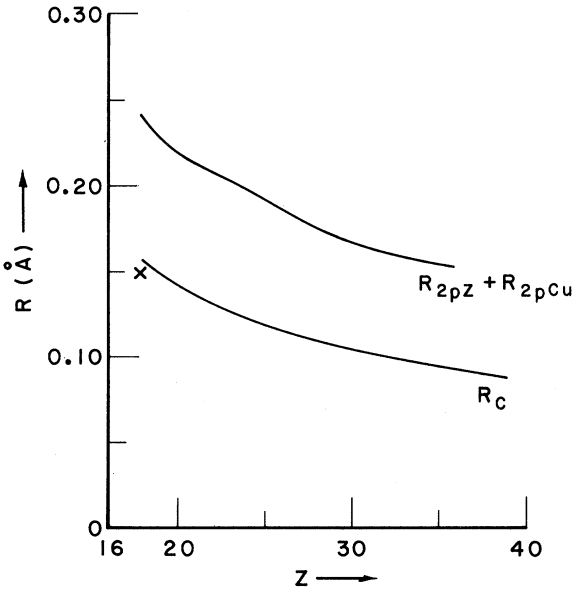

FIG. 14. Comparison of characteristic internuclear distance R_C (obtained from fit to experimental data in Fig. 13) with sum of L-shell radii (obtained from the first reference in Fig. 7, p. 210). The cross is a point obtained from Ref. 16.

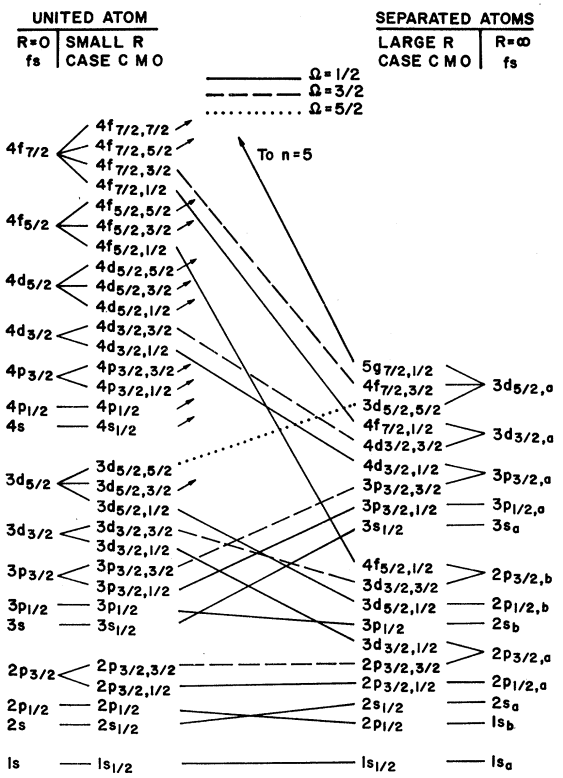

FIG. 15. Correlation diagram for slightly asymmetric atoms with the effect of fine structure shown. See legend to Fig. 10.

$$M = e^{-v_0/v}/(1 + e^{-v_0/v}), \tag{8}$$

v is the relative velocity of the nuclei at infinite separation, and the characteristic velocity is given by $v_0 = \Delta E/2\lambda$, where ΔE is the energy deficit (in a.u.) between the two inner shells (see Fig. 7) and λ is the effective range of the interaction.[44] The characteristic internuclear distance R_C was assumed to be a smoothly varying function of atomic number Z. We also made the reasonable and simplifying assumption that effective range λ and R_C were proportional to each other. The results for R_C are shown in Fig. 14. The effective range was found to have the value

$$\lambda = 0.20 R_C. \tag{9}$$

We get a slightly larger value for λ if we use $v(R_C)$ in (8), rather than $v(\infty)$.

D. Discussion

The value of R_C for the Ar+Cu pair is in good agreement with the data of Saris *et al.*,[16] which they obtained from the reverse experiment, Cu on Ar. Also, the characteristic internuclear distance is about $\frac{2}{3}$ the sum of $L_{II,III}$-shell radii, again

in agreement with the results of Saris,[16] and Fastrup *et al.*[17] The effective range from (9) is in reasonable agreement with the "active" range of internuclear distances found by Fastrup,[17] Everhart and Afrosimov,[10] and their co-workers. For example, in Ar+Ar pairs, (9) gives $\lambda = 0.05$Å, which is about the range of active distances found by a completely different approach.[10,17] It is interesting to contrast the narrow effective range of the double promotion of the $4f\sigma$ MO with the much wider range of single promotion of the $2p\sigma$ MO in HeH^+, where the K-electron-shell radius is the same as the effective range.[44]

E. Other Cases of L-Shell Promotion

Stein *et al.*[58] have measured the inner-shell vacancy production in the quasisymmetric collisions of 30-MeV iodine ions ($Z = 53$) with a Te ($Z = 52$) solid target. It is noteworthy that filling the exit channels $3s$, $3p$, $3d$, $4s$, $4d$, $5s$, and almost all of $5p$ lowers the excitation probability for the $4f\sigma$ MO from 1.0 in lighter atoms to 0.4 in the present case. In gas targets, this probability is much lower, as the "solid effect" is absent as shown recently by Lutz *et al.*[24]

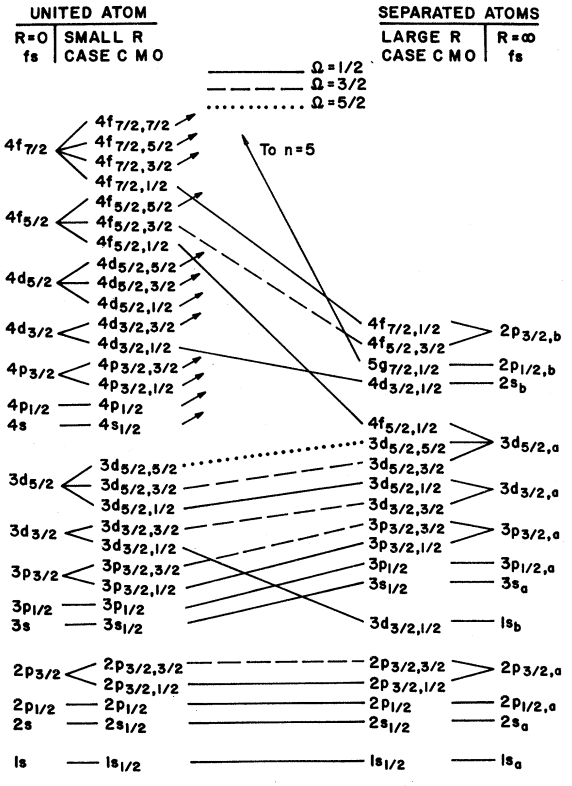

FIG. 16. Correlation diagram with fine structure for the case of swapped energy levels. See legend to Fig. 10.

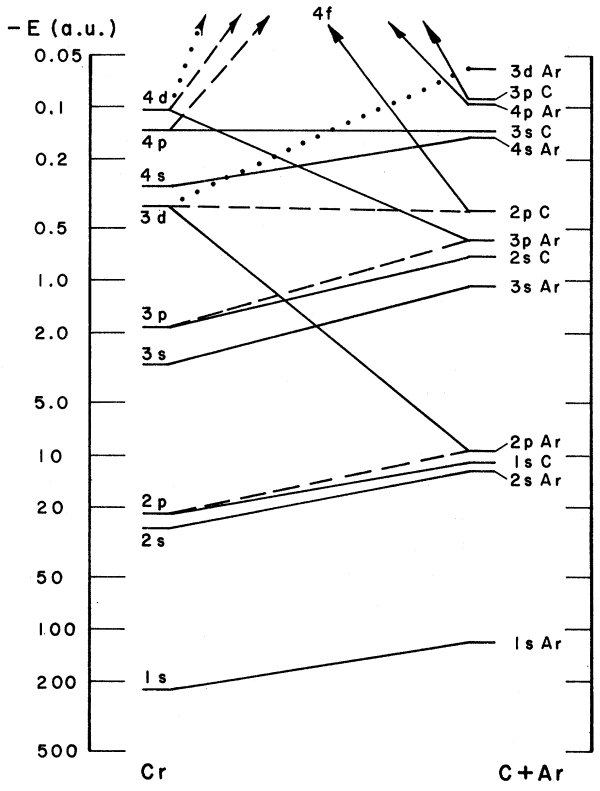

FIG. 17. Carbon-argon correlation diagram. See legend to Fig. 10.

The results of Datz *et al.*[24] were interpreted by them in terms of a molecular promotion effect. It is straightforward to construct correlation diagrams which include spin-orbit coupling. These are given in Figs. 15 and 16. The correlations for $p_{3/2}$ and $p_{1/2}$ levels is quite different, in agreement with the experimental results.[24] However we are presently unable to give a detailed explanation for these results in terms of the promotion model.

IV. K-SHELL PROMOTION

K-shell excitation is particularly simple in the asymmetric case. It can be seen from Fig. 4 and the rules for swapping in Sec. II B that K-shell promotion in all collisions can only occur in the lighter atom. This rule is well substantiated by a host of experiments.[59]

Figure 9 illustrates this for carbon targets and projectiles of different Z. The cross sections for H and He are much smaller than for all other elements. The results for C^+, N^+, O^+ and Ne^+ projectiles show promotion effects [see Secs. II D (iii) and II E] graphically. Except for large energies, these overcome the opposing effect of larger nuclear charges causing increased excitation. Actually one has, respectively 1, 3, 4, and 5 vacancies

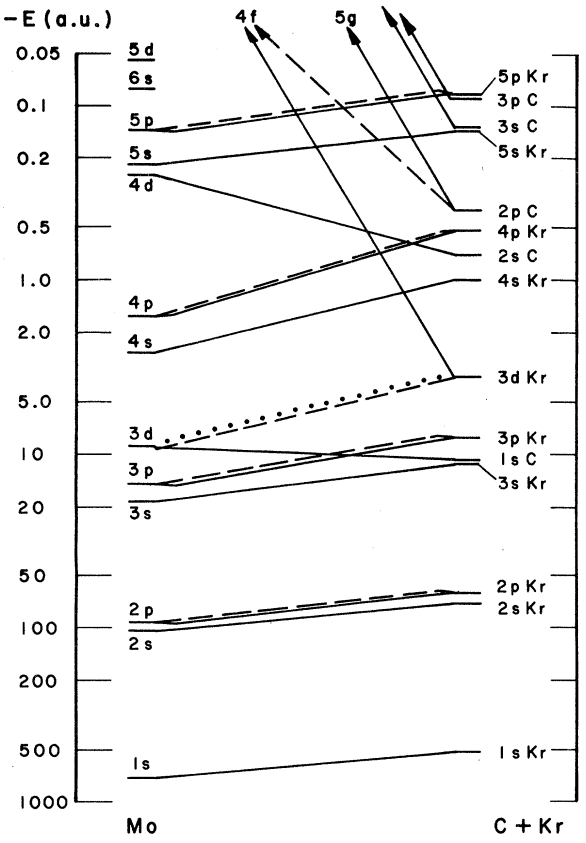

FIG. 18. Carbon-krypton correlation diagram. See legend to Fig. 10.

in the $2p$ shell (Ne^+, O^+, N^+, and C^+ projectiles). (In Fig. 5, a is the projectile and b the carbon target.) Statistically, the number of vacancies in the $2p\pi$ MO, and therefore the probability of excitation, increases as a function of the number of vacancies. Consequently, as shown in Fig. 9, the cross section rises at a given energy from neon to carbon. The very large cross sections for Ar are clearly a level matching effect between $C(K)$ and $Ar(L_{II,III})$ (see Fig. 17). The results for Kr and Xe are inconsistent with the promotion model. In particular, it can be seen from the correlation diagram for C+Kr (Fig. 18) that the $3d$(Kr) exit channels for $C(K)$ shell excitation are closed, except for the solid effect. A more definitive experiment would be to use a gaseous target containing C or Kr to study this system. Because of the level matching between $C(K)$ and $Kr(M_{I,II})$, which the promotion model predicts to be of only weak significance, this experiment would be a particularly crucial test of the model.[60]

Recently, Fortner *et al.*[21] have observed resolved M-shell x rays from Xe projectiles on solid targets with $24 \leq Z \leq 29$. These show clearly the excitation of both collision partners as the Xe M shell swaps with the partner L-shell levels at about $Z = 27$. From Fig. 7, one can see that Xe $3p$ swaps with the partner $2s$ level at this value of Z. In gas-target collisions, one would expect Xe $3d$-target $2p$-level swapping to occur at $Z \sim 25, 26$.

Recently, Der *et al.*[21] have reported pronounced differences between solid- and gas-carbon targets for C K-shell-vacancy production by argon-ion projectiles.

Two interpretations of these experiments are possible. Both views involve the "solid effect," which ionizes and excites the electrons of the projectile. One view holds that the change in promotion is caused by the shift downward of projectile energy levels. The other view points to the opening of exit channels, or other, poorly understood, solid effects. Since both causes would have similar effects in these experiments, neither is definitively ruled out. However we favor the exit channel mechanism (see Sec. II E). A distinction between these two interpretations could be made by using gaseous targets with projectiles with different degrees of ionization.

The practice of some authors[19] is to fit the total cross sections for K-shell excitation with analytical expressions derived from the Landau-Zener model. The crossing radii derived from these fits have no significance, as the excitation is via a level crossing at zero internuclear distance.

ACKNOWLEDGMENTS

One of us (M. B.) wishes to thank Dr. V. Sidis for fruitful discussions of the molecular aspect of this work. We are indebted to S. Datz, B. Fastrup, R. Fortner, K. Taulbjerg, P. Sigmund, and F. Saris for many helpful communications and discussions about their results.

---

*A preliminary account of this work was given by one of us (M. B.) at the Fifth Colloque National sur le Physique des Collisions Electroniques et Atomiques, Rennes, March, 1971; and by both of us at the Second International Seminar on Ion-Atom Collisions and the Seventh International Conference on the Physics of Electronic and Atomic Collisions, Amsterdam, 1971. Hereafter, the latter conference will be abbreviated Seventh ICPEAC.

†Associated with the Centre National de la Recherche Scientifique.

‡This work was supported by a grant from the U. S. National Science Foundation.

[1]F. Hund, Z. Physik 40, 742 (1927).
[2]R. S. Mulliken, Phys. Rev. 32, 186 (1928).
[3]O. Beeck, Ann. Physik 5, 1001 (1930); O. Beeck and J. C. Mouzon, *ibid.* 11, 737 (1931); 11, 858 (1931).
[4]W. Weizel and O. Beeck, Z. Physik 76, 250 (1932).
[5]W. M. Coates, Phys. Rev. 46, 542 (1934).

[6]D. E. Moe and O. H. Petch, Phys. Rev. 115, 349 (1959); 110, 1358 (1958).

[7]N. V. Fedorenko, Zh. Tekh. Fiz. 24, 784 (1954); V. V. Afrosimov and N. V. Federenko, Zh. Tekh. Fiz. 27, 2557 (1957) [Sov. Phys. Tech. Phys. 2, 2378 (1957)].

[8]R. J. Carbone, E. N. Fuls, and E. Everhart, Phys. Rev. 102, 1524 (1956); E. N. Fuls, P. R. Jones, F. P. Ziemba, and E. Everhart, *ibid.* 107, 704 (1957); G. H. Morgan and E. Everhart, *ibid.* 128, 667 (1962).

[9]F. T. Smith, R. P. Marchi, and K. G. Dedrick, Phys. Rev. 150, 79 (1966).

[10]V. V. Afrosimov, Yu. S. Gordeev, M. N. Panov, and N. V. Fedorenko, Zh. Tekh. Fiz. 34, 1613 (1964); 34, 1624 (1964); 34, 1637 (1964); 36, 123 (1966) [Sov. Phys. Tech. Phys. 9, 1248 (1965); 9, 1256 (1965); 9, 1265 (1965); 11, 89 (1966)]; Zh. Eksperim. i Teor. Phys. Pis'ma v Redaktsiya 2, 291 (1966) [Sov. Phys. JETP Letters 2, 185 (1966)]. E. Everhart and Q. C. Kessel, Phys. Rev. Letters 14, 247 (1965); Q. C. Kessel, A. Russek, and E. Everhart, *ibid.* 14, 484 (1965); Q. C. Kessel and E. Everhart, Phys. Rev. 146, 16 (1966); Q. C. Kessel, M. P. McCaughey, and E. Everhart, *ibid.* 153, 57 (1967); Phys. Rev. Letters 16, 1189 (1966); 17, 1170 (1966); Q. C. Kessel, P. H. Rose, and L. Grodzins, *ibid.* 22, 1031 (1969). For a summary of these experiments, see Q. C. Kessel, in *Case Studies in Atomic Collisions Physics I*, edited by E. W. McDaniel and M. R. C. McDowell (North-Holland, Amsterdam, 1969), p. 401; see also Q. C. Kessel, in *Seventh ICPEAC, Invited Talks and Progress Reports*, edited by T. R. Govers and F. J. de Heer (North-Holland, Amsterdam, 1971).

[11]H. W. Berry, Phys. Rev. 121, 1714 (1961); 127, 1634 (1962); R. B. Barker and H. W. Berry, *ibid.* 151, 14 (1966); C. Snoek, R. Geballe, W. F. van der Weg, P. K. Rol, and D. J. Bierman, Physica 31, 1553 (1965); G. Gerber, R. Morgenstern, and A. Niehaus, Phys. Rev. Letters 23, 511 (1969); G. Ogurtsov, I. P. Flaks, and S. V. Avakyan, Zh. Eksperim. i Teor. Fiz. 57, 27 (1969) [Sov. Phys. JETP 30, 16 (1970)]; G. Ogurtsov and Y. Kydin, *ibid.* 57, 1908 (1969) [30, 1032 (1970)]; M. E. Rudd, T. Jorgensen, Jr., and D. J. Volz, Phys. Rev. 151, 28 (1966); Phys. Rev. Letters 16, 929 (1966). For a review, see M. E. Rudd, in *Seventh ICPEAC, Invited Talks and Progress Reports*, edited by T. R. Govers and F. J. de Heer (North-Holland, Amsterdam, 1971).

[12]G. N. Ogurtsov, I. P. Flaks, and S. V. Avakyan, Zh. Tekh. Fiz. 40, 2124 (1970) [Sov. Phys. Tech. Phys. 15, 1656 (1971)]; B. Fastrup and G. A. Larsen, in *Abstracts of Papers of the Seventh ICPEAC*, edited by L. M. Branscomb, H. Ehrhardt, R. Geballe, F. J. de Heer, N. V. Fedorenko, J. Kistemaker, M. Barat, E. E. Nikitin, and A. C. H. Smith (North-Holland, Amsterdam, 1971), p. 392.

[13]G. M. Thomson, P. C. Laudieri, and E. Everhart, Phys. Rev. A 1, 1439 (1970).

[14]G. M. Thomson, P. C. Laudieri, W. W. Smith, and A. Russek, Phys. Rev. A 3, 2028 (1971).

[15]M. E. Cunningham, R. C. Der, R. J. Fortner, T. M. Kavanagh, J. M. Khan, C. B. Layne, E. J. Zaharis, and J. D. Garcia, Phys. Rev. Letters 24, 931 (1970).

[16]F. W. Saris and D. Onderdelinden, Physica 49, 441 (1970); F. W. Saris, *ibid.* 52, 290 (1971); thesis (University of Leiden, 1971) (unpublished); F. W. Saris and D. J. Bierman, Phys. Letters 35A, 199 (1971); for a review, see F. W. Saris, in *Seventh ICPEAC, Invited Talks and Progress Reports*, edited by T. R. Govers and F. J. de Heer (North-Holland, Amsterdam, 1971).

[17]B. Fastrup and G. Hermann, Phys. Rev. Letters 23, 157 (1969); B. Fastrup, G. Hermann, and K. J. Smith, Phys. Rev. A 3, 1591 (1971); see also Ref. 13.

[18]F. W. Bingham, Phys. Rev. 182, 180 (1969); F. W. Bingham and J. K. Rice, Phys. Rev. A 4, 996 (1971).

[19]R. C. Der, R. J. Fortner, T. M. Kavanagh, and J. M. Khan, Phys. Rev. A 4, 556 (1971); R. C. Der, T. M. Kavanagh, J. M. Khan, B. P. Curry, and R. J. Fortner, Phys. Rev. Letters 21, 1731 (1968); R. J. Fortner, B. P. Curry, R. C. Der, T. M. Kavanagh, and J. M. Khan, Phys. Rev. 185, 164 (1969).

[20]T. M. Kavanagh, M. E. Cunningham, R. C. Der, R. J. Fortner, J. M. Khan, J. Zaharis, and J. D. Garcia, Phys. Rev. Letters 25, 1473 (1970).

[21]R. J. Fortner, R. C. Der, and T. M. Kavanagh, Phys. Letters 37a, 259 (1971); R. J. Fortner (private communication).

[22]V. V. Afrosimov, Yu. S. Gordeev, M. N. Panov, and N. V. Fedorenko, Zh. Tekh. Fiz. 36, 123 (1966) [Sov. Phys. Tech. Phys. 11, 89 (1966)].

[23]V. V. Afrosimov, Yu. S. Gordeev, A. M. Polyansky, and A. P. Shergin, in *Seventh ICPEAC, Invited Talks and Progress Reports*, edited by T. R. Govers and F. J. de Heer (North-Holland, Amsterdam, 1971), p. 397.

[24]B. Fastrup, G. Hermann, and Q. Kessel, in *Seventh ICPEAC, Invited Talks and Progress Reports*, edited by T. R. Govers and F. J. de Heer (North-Holland, Amsterdam, 1971), p. 390; B. Fastrup and G. A. Larsen, *ibid.*, p. 392, P. Dahl and D. C. Lorents, *ibid.* p. 395; S. Datz, C. D. Moak, B. R. Appleton, M. D. Brown, and T. A. Carlson, *ibid.*, p. 409; M. Terasawa, T. Tamura, and H. Kamada, *ibid.*, p. 416; H. O. Lutz, J. Stein, S. Datz, and C. D. Moak, Phys. Rev. Letters 28, 8 (1972).

[25]H. J. Specht, Z. Physik 185, 301 (1965). Dr. P. Armbruster has kindly pointed out that this was a continuation of his work [P. Armbruster, Z. Physik, 166, 341 (1962); P. Armbruster, E. Roeckl, H. J. Specht, and A. Vollmer, Z. Naturforsch. 19a, 1301 (1964)].

[26]To our knowledge the first such calculation to show promotion of inner-shell electrons is by E. W. Thulstrup and H. Johansen, in *Seventh ICPEAC, Invited Talks and Progress Reports*, edited by T. R. Govers and F. J. de Heer (North-Holland, Amsterdam, 1971), p. 118; Phys. Rev. (to be published).

[27]W. Lichten, Phys. Rev. 131, 229 (1963).

[28]U. Fano and W. Lichten, Phys. Rev. Letters 14, 627 (1965).

[29]W. Lichten, Phys. Rev. 164, 131 (1967).

[30]See the 1962 paper by Berry, Ref. 11; L. M. Kishinevsky and E. S. Parillis, in *Proceedings of the Fifth ICPEAC* (Nauka, Leningrad, 1967), p. 100; V. V. Afrosimov, Yu. S. Gordeev, A. M. Polyanskii, and A. P. Shergin, Zh. Eksperim. i Teor. Fiz. 57, 806 (1969) [Sov. Phys. JETP 30, 441 (1970)].

[31]F. T. Smith, D. C. Lorents, W. Aberth, and R. P. Marchi, Phys. Rev. Letters 15, 742 (1965); M. Barat, J. Baudon, M. Abignoli, and J. C. Houver, J. Phys. B 3, 230 (1970); V. V. Afrosimov, Y. S. Gordeev, A. M. Polyansky, and A. P. Shergin, in Fifth ICPEAC, Ref. 30, p. 89; P. Loftager and G. Claussen, in *Proceedings of the Sixth ICPEAC* (M. I. T. Press, Cambridge, 1969), p. 518; V. V. Afrosimov, Yu. S. Gordeev, V. K. Nikulin, A. M. Polyansky, and A. P. Shergin, in *Seventh ICPEAC,*

InvitedTalks and Progress Reports, edited by T. R. Govers and F. J. de Heer (North-Holland, Amsterdam, 1971), p. 149; see also Ref. 22.

[32]See all papers after 1965 referred to in Refs. 11–14.

[33]H. Rosenthal and H. M. Foley, Phys. Rev. Letters 23, 1480 (1969); H. Rosenthal, Phys. Rev. A 4, 1030 (1971).

[34]S. Dworetsky, R. Novick, W. Smith, and N. Tolk, Phys. Rev. Letters 18, 939 (1967); M. Lipeles, R. Novick, and N. Tolk, *ibid.* 15, 815 (1965); N. H. Tolk, C. W. White, S. H. Dworetsky, and L. A. Farrow, *ibid.* 25, 1251 (1970); N. H. Tolk, C. W. White, S. H. Dworetsky, and D. L. Sims, in *Seventh ICPEAC, Invited Talks and Progress Reports*, edited by T. R. Govers and F. J. de Heer (North-Holland, Amsterdam, 1971, p. 584; S. H. Dworetsky and R. Novick, Phys. Rev. Letters 23, 1484 (1969); L. Wolterbeek-Muller and F. J. de Heer, Physica 48, 345 (1970); S. V. Bobashev, Zh. Eksperim. i Teor. Fiz. Pis'ma v Redaktsiya 11, 389 (1970) [Sov. Phys. JETP Letters 11, 260 (1970)]; S. S. Pop, I. Yu. Krivsky, I. P. Zapesochny, M. V. Baletskaya, Zh. Eksperim. i Teor. Fiz. 59, 696 (1970) [Sov. Phys. JETP 32, 380 (1971)]; C. V. Bobashev, B. A. Kritskii, Zh. Eksperim. i Teor. Fiz. Pis'ma Redaktsiya 12, 280 (1970) [Sov. Phys. JETP Letters 12, 189 (1970)]; V. A. Ankudinov, S. V. Bobashev, and V. I. Perel, in *Seventh ICPEAC Invited Talks and Progress Reports*, edited by T. R. Govers and F. J. de Heer (North-Holland, Amsterdam, 1971), p. 581; Zh. Eksperim. i Teor. Fiz. 60, 906 (1971) [Sov. Phys. JETP 33, 490 (1971)]; N. H. Tolk, C. W. White, S. H. Dworetsky, and D. L. Simms, in *Seventh ICPEAC, Invited Talks and Progress Reports*, edited by T. R. Govers and F. J. de Heer (North-Holland, Amsterdam, 1971), p. 584; I. P. Zapesochny and S. S. Pop, *ibid.*, p. 591; O. B. Shpenik, I. P. Zapexochny, and A. N. Zavilopuio, *ibid.*, p. 594; D. H. Jaecks, W. de Rijk, and P. J. Martin, *ibid.*, p. 605; Z. Z. Latypov and A. A. Shaporenko, Zh. Eksperim. i Teor. Fiz. Pis'ma v Redaktsiya 13, 525 (1971); 12, 177 (1971) [Sov. Phys. JETP Letters 13, 375 (1971); 12, 123 (1970)].

[35]D. C. Lorents and G. M. Conklin (unpublished); also, in *Seventh ICPEAC, Invested Talks and Progress Reports*, edited by T. R. Govers and F. J. de Heer (North-Holland, Amsterdam, 1971), p. 130. These authors also independently extended the promotion model to K-shell excitation in asymmetric collisions. We are indebted to them for communication of results prior to publication. See also R. Francois, D. Dhuicq, and M. Barat (unpublished). In these two papers, the difficulties arising in the application of the promotion model to outer-shell excitations are pointed out.

[36]F. T. Smith, Phys. Rev. 179, 111 (1969); B. A. Lippmann and T. F. O'Malley, Phys. Rev. A 2, 2115 (1970); T. F. O'Malley, Phys. Rev. 150, 14 (1966); 162, 98 (1967); T. F. O'Malley and H. S. Taylor, *ibid.* 176, 207 (1968); V. Sidis and H. LeFebvre-Brion, J. Phys. B 4, 1040 (1971); B. Andresen and S. E. Nielsen, Mol. Phys. 21, 523 (1971); see also R. D. Levine, B. R. Johnson, and R. B. Bernstein, J. Chem. Phys. 50, 1694 (1969). At present the problem of constructing a diabatic basis set has only been studied for Σ-Σ coupling, i.e., for collisions in which there is no rotational coupling. The problem here is that slow collisions are adiabatic for radial coupling; these collisions are diabatic for rotational coupling.

[37]P. M. Morse and E. Stückelberg, Phys. Rev. 33, 932 (1929); see also H. Bethe, in *Handbuch der Physik*, edited by H. Geiger and K. Scheel (Springer-Verlag, Berlin, 1933), Vol. XXIV, Pt. I, pp. 524–534.

[38]D. R. Bates and T. R. Carson, Proc. Roy. Soc. (London) A234, 207 (1956).

[39]S. S. Gershtein and V. D. Krivchenkov, Zh. Eksperim. i Teor. Fiz. 40, 1491 (1961) [Sov. Phys. JETP 13, 1044 (1961)]; K. Helfrich and H. Hartmann, Teoret. Chim. Acta 16, 263 (1970).

[40]$n_3 = n_\phi$ is the magnetic quantum number, equal to the component of the angular momentum along the internuclear axis. However, if real functions are used, n_ϕ is the number of nodal surfaces.

[41]This holds for all such diagrams in this article, except Figs. 1–3.

[42]L. I. Ponomarev and T. P. Puzynina, Zh. Eksperim. i Teor. Fiz. 52, 1273 (1967) [Sov. Phys. JETP 25, 846 (1967)].

[43]Table I in Ref. 29 is still valid, except that MO parity is no longer conserved, except for crossing near the UA limit. See Sec. II B of this paper. It should be mentioned that the MO of Ref. 36 (Sidis and LeFebvre-Brion) are constructed to eliminate some of these interactions while the total energy curves may cross.

[44]W. Lichten, Phys. Rev. 139, A27 (1965).

[45]Later, Sec. IID, a similar discussion is given of the case of nearly degenerate levels in the quasisymmetric case.

[46]J. D. Garcia, Phys. Rev. A 1, 280 (1970); 3, 955 (1971); E. Merzbacher, H. W. Lewis, in *Encyclopedia of Physics*, edited by S. Flügge (Springer-Verlag, Berlin, 1958), Vol. 34, p. 166; J. M. Hansteen, International Seminar on Ion-Atom Collisions, 1971 (unpublished).

[47]For a more detailed discussion of these excitation mechanisms, see Refs. 28 and 29. For more detailed applications, see Sec. III of this paper.

[48]See Ref. 44 and Secs. IIB and III of this paper.

[49]M. P. McCaughey, E. J. Knystautas, H. C. Hayden, and E. Everhart, Phys. Rev. Letters 21, 65 (1968). In the case of 2s vacancies in (Ar^{++} or Ar) on Ar at 15 keV, Ogurtsov *et al.* find the expected ratio of 2:1 (see Sixth ICPEAC, Ref. 31, p. 274).

[50]B. Fastrup, G. Hermann, and Q. C. Kessel, Phys. Rev. Letters 27, 771 (1971). These authors independently extended the promotion model to cover the case of asymmetric K-shell promotion. It should be noted that the other factors mentioned earlier in this section, also tend to raise the x-ray yields in going from Ne^+ to C^+ projectiles (see Fig. 9 and Ref. 19).

[51]R. K. Cacak, Q. C. Kessel, and M. E. Rudd, Phys. Rev. A 2, 1327 (1970); Q. C. Kessel, Bull Am. Phys. Soc. 14, 946 (1969).

[52]However it should be noted that the double quantum transition to the $3d\delta$ levels is open for all values of Z in this experiment.

[53]Q. C. Kessel, in Fifth ICPEAC, Ref. 30, p. 92.

[54]E. J. Knystautas, Q. C. Kessel, R. Del Boca, and H. C. Hayden, Phys. Rev. A 1, 825 (1970).

[55]The $3p\sigma$-$3p\pi$ mechanism, however, should not be effective here.

[56]These arguments hold for the case that both collision partners are atoms. For solid targets, atomic levels are split into bands that are mixtures of atomic orbitals. In this region of the Periodic Table ($Z \gg 30$, it is likely that the bands do not consist of mixtures of $n=3$ orbitals with other shells. In general, only valence-shell atomic or-

bitals are mixed with orbitals of different principal quantum number. Band mixing is too small to mix inner shells with each other.

[57]E. Everhart, G. Stone, and R. J. Carbone, Phys. Rev. 99, 1287 (1955).

[58]H. J. Stein, H. O. Lutz, P. H. Mokler, K. Sistemich, and P. Armbruster, Phys. Rev. A 2, 2575 (1970); Phys. Rev. Letters 24, 701 (1970).

[59]For a review of the literature, see W. Brandt and R. Laubert, Phys. Rev. Letters 24, 1037 (1970).

[60]K. Taulbjerg and P. Sigmund [Phys. Rev. A 5, 1285 (1972)] have shown that the cross sections for carbon K-shell excitation by Kr and Xe ions (see Fig. 9) are spuriously high, because of recoil effects. This removes a serious discrepancy between experimental results and the promotion model. These authors also have pointed several other "solid effects" which limit the validity of experiments using solid targets.

PHYSICAL REVIEW A VOLUME 6, NUMBER 1 JULY 1972

Charge States of 29.2- to 45.7-MeV Uranium Ions Emerging from Solid Foils*

M. D. Brown†
Oak Ridge National Laboratory, Oak Ridge, Tennessee 37830
(Received 30 November 1971)

The equilibrium-charge-state distributions of uranium ions have been measured in carbon at 29.2 and 45.7 MeV, in aluminum at 29.1 MeV, in silver at 29.7 MeV, and in gold at 29.6 MeV (energy is the exit-beam energy). Following the passage of monoenergetic uranium ions from the Oak Ridge tandem accelerator through each thin-foil target, the charge states in the emergent beams were spatially separated in an electrostatic analyzer and measured with a position-sensitive surface-barrier detector. The foil thicknesses, derived from α-particle energy-loss measurements, were 34 $\mu g/cm^2$ for carbon, 51 $\mu g/cm^2$ for aluminum, 58 $\mu g/cm^2$ for silver, and 110 $\mu g/cm^2$ for gold. Non-Gaussian charge-state distributions were observed. The most probable charge states are in reasonable agreement with published semiempirical formulas, although some deviations are noted.

I. INTRODUCTION

The capture and loss of electrons by partially stripped heavy ions are among the most common processes occurring during the passage of these ions through matter. Many experimental determinations of equilibrium- and nonequilibrium-charge-state distributions have been reported, mostly for the lighter ions.[1-10] Theoretical calculations of these distributions are dependent on a number of simplifying assumptions.[11-13] Available semiempirical formulas[14,15] are generally able to predict the average charge to within ± 1 charge state in cases for which shell effects,[16] excitation processes,[17,18] and target z dependence are not of overriding importance. Since it is desirable to know the range of validity for these formulas and to discover the physical reasons for their occasional failure, deviations from the formulas are worthy of experimental study.

The equilibrium-charge-state distributions and the approach to equilibrium are topics of interest for several other reasons. The relation between stopping processes and projectile charge states can be studied. Heavy-ion-accelerator design requires more knowledge of heavy-ion charge-state distributions than is presently available. The energy-dependent proportionality between beam current and particle flux is frequently of considerable practical interest to the experimentalist. Relative ionic-charge-state populations often enter into considerations of atomic spectral line intensities in plasma physics, beam-foil spectroscopy, and astrophysics.

The published experimental literature concerning ions as heavy as uranium is sparse. Betz *et al.*[14] reported the first uranium-charge-state distributions, using air and Formvar targets with beam energies in the range from 10 to 70 MeV. Grodzins *et al.*[19] later reported charge-state data for uranium in carbon over the energy range 30–150 MeV. Recently, Wittkower and Betz[20] reported uranium-charge-state distributions for the gases H_2, He, N_2, O_2, Ar, Kr, and Xe, and for foils of carbon and gold at energies from 2 to 15 MeV. In the present investigation, charge fractions were obtained in carbon at 29.2 and 45.7 MeV, in aluminum at 29.1 MeV, in silver at 29.7 MeV, and in gold at 29.6 MeV (emergent-uranium-beam energy).

II. EXPERIMENTAL PROCEDURE

Single-component beams of 30.2-MeV U^{8+} and 47.3-MeV U^{10+} were obtained from the Oak Ridge tandem Van de Graaff accelerator by stripping 30.2-MeV U^{5+} and 47.3-MeV U^{7+} beams, respectively, in a gas cell located upstream of the analyzing magnet (see Fig. 1). Negative molecular ions contain-